DESIGN AND EVALUATION OF DISTRIBUTED ELECTRIC DRIVE ARCHITECTURES FOR HIGH-LIFT CONTROL SYSTEMS

T. Lampl, R. Königsberger and M. Hornung
Institute of Aircraft Design, Technical University of Munich
Boltzmannstraße 15, 85748 Garching, Germany

Abstract

High-lift control systems of commercial transport aircraft increase lift during low speed phases and keep the landing speed in reasonable limits. Today's high-lift control systems consist of leading and trailing-edge devices which are actuated over established mechanical transmission shafts driven by central power control units. With the ongoing trend of more-electric aircraft and potential benefits by functional enhancement of the flight control system, new possibilities arise for future high-lift system architectures. One promising approach is a distributed electric drive architecture. This provides the opportunity to enable advanced high-lift control systems with multifunctional control surfaces driven by electrical actuators. In this contribution, a conventional high-lift system architecture - which serves as a reference system – and three distributed system architectures using electrical actuators are developed. The trailing-edge actuation system has been chosen as a representative example for this study. The system architectures are developed in an iterative design process to fulfill the high-lift system requirements, and comply with the safety regulations. Furthermore, the system masses and operating costs are estimated to evaluate the different system architectures. Finally, it can be stated, that distributed system architectures show advantages regarding overall system mass and direct operating costs compared to the conventional, reference system architecture.

1 INTRODUCTION

The introduction of jet engines in civil aviation lead to a significant increase in cruise speed. This was accomplished by wing sweep and the introduction of super-critical airfoils. Further performance optimizations led to increased wing loading and thus higher lift coefficients at low speeds provided by high-lift systems were required, to keep landing speed and runway distances in reasonable limits [1]. Figure 1 shows the evolution of high-lift systems of commercial transport aircraft (Airbus and Boeing). It can be observed, that the complexity of the high-lift system – regarding the inboard and outboard trailing-edge flaps – has been continuously reduced in the last 25 years.
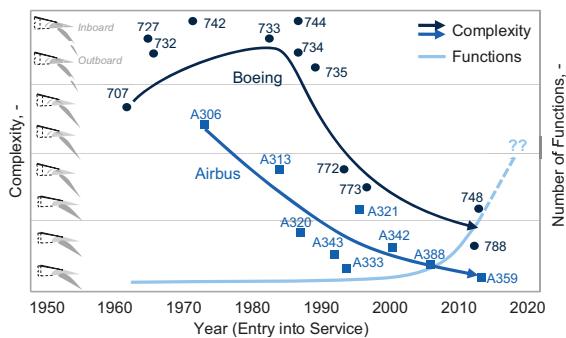

FIGURE 1. Evolution of high-lift systems of commercial transport aircraft, modified from Recksiek [1].

Moreover, due to the optimization during the last decades, a plateau in terms of benefits on aircraft level has been reached. The state-of-the-art actuation system of the high-lift devices still consists of a mechanical transmission shaft

driven by centrally located Power Control Units (PCUs). This assures a synchronous deployment of all high-lift devices on the left and right wing, but prevents functional flexibility [1]. Nevertheless, the latest introduced transport aircraft – the Airbus A350 and Boeing 787 – provide additional control functions by the trailing-edge flaps, see Figure 2. The Cruise Variable Camber (CVC) function allows the aerodynamic improvement of the wing during cruise. The Differential Flap Setting (DFS) function enables the wing load control to save wing structure mass. Beside the means of functional enhancement, the trend towards More-Electric Aircraft (MEA) with the evolutionary application of enabling electrical technologies leads to considerable changes on aircraft system level. Therefore, a lot of development effort is put into MEA concepts and technologies [3–6].
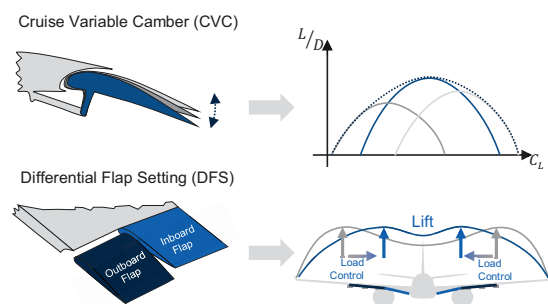

FIGURE 2. Multifunctional use of the trailing-edge flaps for further improvements [2].

Considering MEA technologies and functional enhancements of high-lift control devices, system architectures with distributed electrical flap actuators represent a further leap in high-lift system technology regarding aircraft performance optimization and efficiency improvements [1]. These

advanced high-lift system architectures show potential benefits in terms of system mass and direct operating cost savings, as well as enabling the multifunctional use of the flaps. Furthermore, improvements at the design-engineering, manufacturing and assembly are expected [1,5,7].

The objective of this study is to develop different system architectures with distributed electric drives for high-lift control devices. For each distributed electric drive architecture two types of actuators – the Electro-Mechanical Actuator (EMA) and the Electro-Hydrostatic Actuator (EHA) – are considered, leading to several possible architecture concepts. All developed concepts must fulfill the specified safety, certification, and actuation requirements. To have a basis for the analysis and evaluation a reference aircraft is defined, including a conventional actuation architecture for the high-lift control system. The different system architectures are analyzed in terms of system safety and reliability (FHA, FTA), system mass and costs. Finally, the three designed architectures are compared to the reference architecture to evaluate the benefits of each concept.

2 BACKGROUND

2.1 State of the Art

The main design requirements of the high-lift system architecture of commercial transport aircraft is to assure synchronous setting and to avoid asymmetric flap and slat deflections. Consequently, conventional system architectures with central Power Control Units (PCUs) and mechanical transmission shaft with rotary or ballscrew actuators have been established. Figure 3 shows a representative high-lift system architecture of the Airbus A320, with two drive systems.
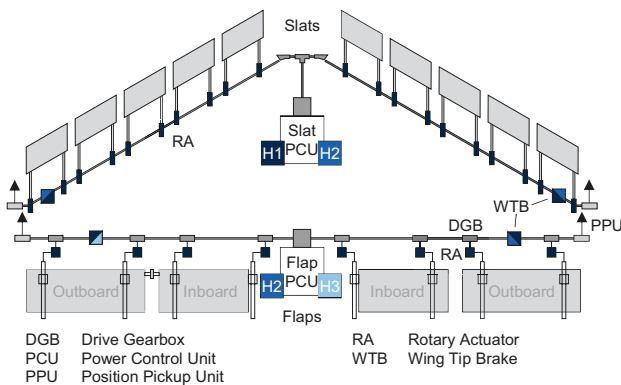

FIGURE 3. Simplified high-lift system architecture of the Airbus A320, modified from Wild [8].

Each drive system consists of two similar hydro-mechanical systems. The PCUs consist of two hydraulic motors and are supplied by the hydraulic power circuits H1, H2 or H3. The mechanical transmission shaft system consists of a high number of components (see Figure 3):

- Differential Gearboxes (DGBs)
- Rotary Actuators (RAs) operate the slats and flaps
- Wing Tip Brakes (WTBs) to prevent asymmetric operation
- Position Pick-Up Units (PPUs) to monitor the system and to detect asymmetric operation

Furthermore, right-angle gearboxes and kink gearboxes at the wing kink are necessary for larger direction changes of the transmission shaft (not shown).

Summarized it can be stated, that conventional high-lift system architectures are rather complex and heavy and prevent the integration of additional control functions. Furthermore, the mechanical transmission shaft system requires high engineering, installation and maintenance effort.

2.2 Advanced High-Lift Control Systems

Various research studies see potential benefits of advanced high-lift systems for commercial transport aircraft by functional enhancement of the flight control systems using multifunctional flight control devices [1,2,6,9,10]. Therefore, a high-lift system architecture with distributed electrical drives will offer the capability for implementation of additional control functions, especially for the trailing-edge devices [1]. In a previous work of Bennett et al. [6], a full-scale demonstrator of distributed electrical flap system with EMAs has been built and successfully tested. Furthermore, according to Christmann et al. [7], distributed flap actuation systems have much lower system inertia and higher stiffness than architectures with a large mechanical transmission shaft powered by a central PCU.

Potential Benefits

A high-lift system with distributed electric drives has potential benefits resulting from the unique system architectures and its characteristics. Please note, that the largest benefit is gained, if all systems on aircraft level are designed for the MEA approach. The main expected advantages of high-lift system architectures with distributed electrical actuators are listed below:

- Increased functionality
- Reduced system mass
- Reduced maintenance
- Reduced energy consumption (power on demand)
- Improved manufacturing and assembly

Challenges

However, in comparison to conventional high-lift systems with transmission shaft, distributed system architectures have more components acting in parallel and therefore require a level of redundancy and fault tolerance to meet the safety and reliability requirements [6].

2.3 Electric Actuator Technologies

The electrical actuators with high power density are the key feature of distributed system architectures. Today, two basic types of actuators are already used for flight control system actuation, which are suitable for distributed electric actuation systems: The Electro-Hydrostatic Actuator (EHA) and the Electro-Mechanical Actuator (EMA).

Electro-Hydrostatic Actuators (EHA)

The EHA is a hybrid electrical and hydraulic device in a self-contained unit. The actuator uses a hydraulic ram to move the flight control device. The EHA is supplied from the electrical power system and the control and monitoring unit sends the input signals to the actuator control electronics.

Furthermore, the EHA uses state-of-the-art power electronics and control techniques to provide more efficient flight control actuation [11].
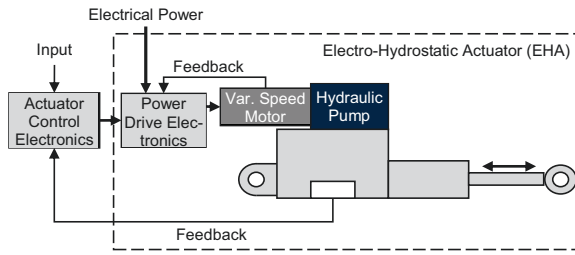

FIGURE 4. Schematic design of an Electro-Hydrostatic Actuator (EHA), modified from [11].

In contrast to conventional, servo-controlled hydraulic actuators, the EHA only draws significant electrical power, when it is required for actuation [11]. Recently, EHAs are partly used for the flight control system of the Airbus A380 and A350.

Electro-Mechanical Actuator (EMA)

The EMA directly converts the electric energy into mechanical motion. Therefore, the electro-hydraulic actuator of the EHA is replaced by an electric motor and a gearbox to move the screwjack actuator, see Figure 5. Generally, the actuation rates of the EMAs are slower than actuation rates of the EHAs, but should be within the required limits for high-lift control systems.
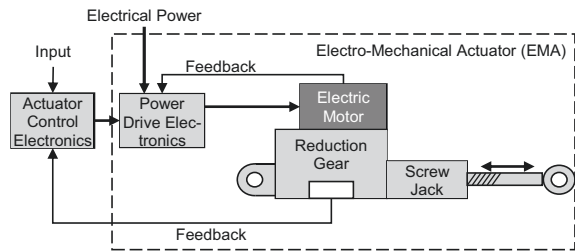

FIGURE 5. Schematic design of an Electro-Mechanical Actuator (EMA), modified from [11].

The biggest disadvantage of the EMA is actuator jamming, causing a failure to the system. In a high-lift system this failure condition is not as critical as for primary flight controls – the aircraft can still be landed safely with degraded performance (higher landing speed).

3   SYSTEM DESIGN METHOD

The development of a high-lift system is an iterative approach between system concept design and safety assessment. The process that is generally recommended for aircraft system design is described by the standard SAE ARP 4754 [12]. The process of system safety assessment is outlined in the standard SAE ARP 4761.

These two processes will be iteratively executed to derive a suitable system that fulfills all requirements and complies with the certification regulations. That simplified interaction of the system development process and the safety assessment is illustrated in Figure 6. The steps performed in this study are highlighted and numbered from 1 to 4.
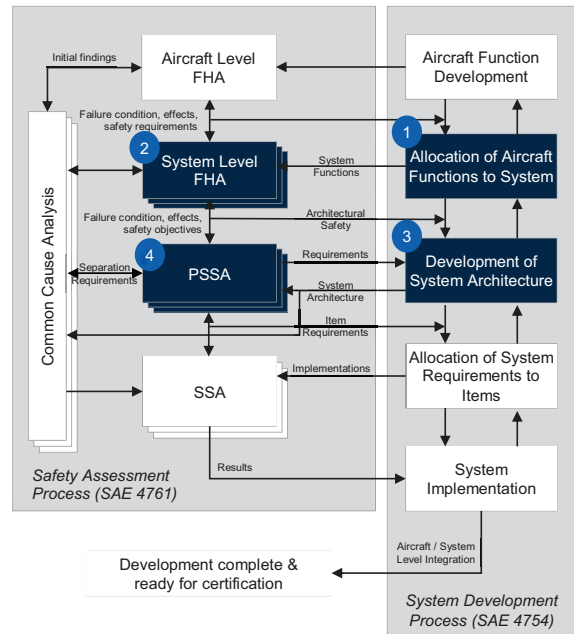

FIGURE 6. Simplified aircraft system development and safety assessment process, modified from SAE [12].

3.1   Reference Aircraft and System Boundary

The reference aircraft is a generic aircraft representing typical twin-engine, medium-range transport aircraft in the size of an Airbus A320 or a Boeing 737. Table 1 gives an overview on the main aircraft data required for this study. The high-lift control system of the reference aircraft consists of 5 slats and 2 flaps on each wing. Since the focus in this study is on the trailing-edge flaps, the main specifications are given in Table 2.

TABLE 1. Main parameters of the reference aircraft.

Parameter	Value	Unit	Parameter	Value	Unit
General			*Wing and High-Lift*		
Capacity (max.)	180	-	Reference Area	122	m²
Length	38	m	Span	34	m
MTOM	75000	kg	Sweep	25	°
Design Range	6000	km	No. Slats	5/5	-
Cruise speed (Ma)	0.78	-	No. Flaps	2/2	-

TABLE 2. Main parameters of the trailing-edge flaps.

Parameter	Inboard	Outboard	Unit
Flap panel area	3.71	4.97	m²
Flap span	3.75	6.10	m
MAC of the flap	0.99	0.83	m
MAC of the wing (@flap position)	5.55	4.60	m
Max. flap deflection angle	40.0	40.0	°
Max. flap extended speed	170	170	kts
Actuator positions (from centerline)	2.0/4.5	7.4/10.5	m

The reference kinematic of the flap actuation is a link-track type kinematic as used on the Airbus A320, see Figure 7. The flap is mounted on a roller carriage which is actuated over the drive/flap link arm to move on the flap track. This link-track kinematics allows for a suitable fowler motion at lower takeoff flap angles and requires very low actuation power [13].

If linear actuators (EHA or EMA) are used, the actuators act directly on the joint between the drive link and flap link arm (see the marked position in Figure 7).
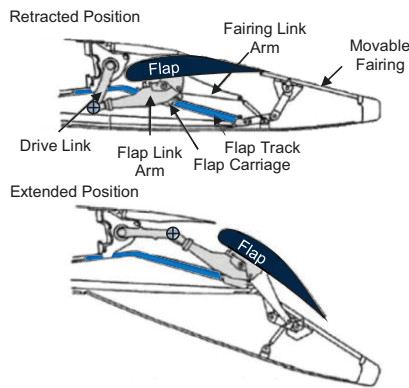

FIGURE 7. Schematic of the Airbus A320 link-track kinematics for trailing-edge flaps, modified from [14].

For the design and evaluation of the system architectures, clear system boundaries should be defined, see Figure 8.
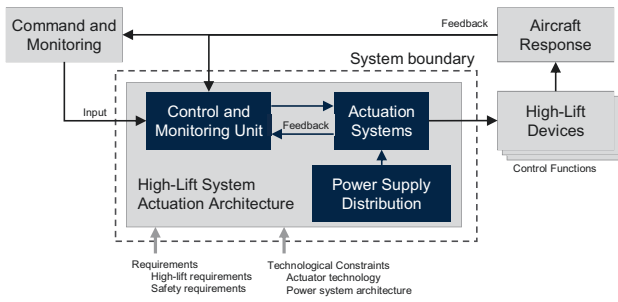

FIGURE 8. Schematic high-lift system actuation architecture (top level) and the system boundary.

The main subsystems of the high-lift system actuation architecture consist of the control and monitoring unit, the actuation system, and the power supply distribution. The power supply systems on aircraft level is not considered. The control and monitoring unit is assumed as a generic black box without modeling their specific functions. The system boundary towards the high-lift devices (structure) is set at the link between the actuators and the linkage of the structural components of the high-lift devices down the load path.

3.2 High-Lift System Requirements

Beside the purpose of the high-lift system to provide additional lift during low speed phases (take-off and landing), the high-lift system of a commercial transport aircraft should fulfil several other multidisciplinary requirements:

- Structural requirements
- Safety and reliability
- Low system mass and complexity
- Low manufacturing and operating costs
- System actuation: speed and power

Since this study focuses on the high-lift system architecture, aerodynamic and structural requirements are not considered. Therefore, the main effort is on certification and safety

requirements, and on the actuation system requirements.

Certification and Safety Requirements

Commercial transport aircraft must comply with the respective certification regulations CS-25 published by the European Aviation Safety Agency (EASA) [15]. The relevant paragraphs §671 to §703 regarding the flight control system can be found in subpart D. Furthermore, §1309 addresses the safety of any aircraft system and its impact on aircraft level. Table 3 gives some guidance on the classification of a failure condition and the associated failure severity and failure probability objectives.

TABLE 3. Safety objectives, according to EASA [15].

Failure Classification	Probability per FH*	Effects on aircraft, passengers and crew
No	No probability	- No effects
Minor	$< 10^{-3}$	- Flight reduction in functional capabilities or safety - Slight increase in crew workload - Physical discomfort for passengers
Major	$< 10^{-5}$	- Significant reduction in functional capabilities, safety - Significant increase in workload or physical discomfort - Physical distress, possible injuries for passengers
Hazardous	$< 10^{-7}$	- Large reduction in functional capabilities or safety - Physical distress or excessive workload of the crew - Serious or fatal injury of passengers or cabin crew
Catastrophic	$< 10^{-9}$	- Hull loss of the aircraft - Multiple fatalities - All failure conditions preventing safe flight or landing

* Flight Hour

At the beginning of the system development, the safety assessment process starts with a Functional Hazard Assessment (FHA). This top-down analysis identifies all safety relevant functions of the aircraft and classifies their possible failure conditions by severity. The assessment is done on aircraft level and system level. On aircraft level the top-level functions are identified. Afterwards, the system-level FHA investigates the effects of system failure conditions on the identified aircraft-level functions. Finally, the failure conditions are classified, according to CS-25 §1309 [15].

During the system development, the results of the FHA are compared to the Preliminary System Safety Assessment (PSSA). The PSSA is a systematic examination of the proposed system architecture to evaluate how failures can lead to the functional hazards identified by the FHA. The FHA is performed for the high-lift control actuation system of the reference aircraft. In a first step, following main functions could be identified:

- High-lift control to provide increased lift during take-off, approach and landing
- Position/actuation indication of the high-lift control devices (e.g. slats, flaps)
- Multifunctional control to provide additional control functions

Based on the identified functions, the failure conditions can be derived and the severity of each failure condition is assessed within the FHA. The results of the FHA are summarized in Table 4. The system safety requirements can be derived from the FHA results. No failure of the described functions may occur in the system with a higher probability as the safety objectives for the failure severity shown in Table 3. The expected failure probability for each function

needs to be evaluated for each system architecture in an individual Fault Tree Analysis (FTA).

TABLE 4. Results of the functional hazard assessment.

Functions	Failure Condition	Flight Phase	Effect of Failure	Classification
High-lift control to provide augmented lift during take-off, approach, landing	High-lift system runaway above max. flap extended speed	All phases	- Structural damage - Loss of control	Catastrophic
	High-lift system runaway below max. flap extended speed	Take-off, Landing	- Reduced flight performance - Deviation from flight path - Significant increase in workload	Hazardous
	High-lift system asymmetry on extension/retraction	Approach/ Climb out	- Loss of control	Catastrophic
Multifunctional control to provide additional functions	Uncommanded retraction of high-lift system	Landing	- Increase of stall speed - Loss of control	Catastrophic
	Loss of extension capability of high-lift system	Landing	- Increase in landing distance - Increase in stall speed	Major
	Loss of retraction capability of high-lift system	Take-off, Climb out	- Reduction in climb performance - Reduced speed and range	Major
	Panel skew	Cruise, Landing	- Reduced aircraft performance - Increase in landing distance - Increase in stall speed	Major
	Multifunctional excessive asymmetry	All phases	- Loss of control	Catastrophic
Position indication of the high-lift system	Loss of position indication	All phases	- Mission cancelation - Increase in landing distance - Increase in stall speed	Major
	Misleading position indication	Take-off, Landing	- Aircraft may approach stall regime without crew recognition	Hazardous

Actuation System Requirements

The developed high-lift actuation system should fulfill requirements for actuation speed, actuation force and power, and frequency response of actuation.

The required actuation speed of the system is derived from the desired time for full extension or retraction of the high-lift control devices. It is assumed that the extension/retraction times of the flaps for high-lift purposes of the distributed system concepts are in the order of 30 seconds – comparable to the extension/retraction times of conventional high-lift systems. To calculate the actuator speeds, data of the Airbus A320 from the work of Chaves-Vargas [16] serve as a reference. Therefore, an angular speed of the rotary actuator of approximately 3.6°/s is required. For linear actuators with an assumed stroke of about 520mm, an actuation speed of 17mm/s can be estimated.

The required actuation force depends on the respective aerodynamic loads and on the actuation system (kinematics). A hinged control surface should overcome the hinge moment due to aerodynamic forces. For a more complex

fowler kinematic the relationship of the aerodynamic load and required force of the actuator strongly depends on the selected kinematics. To estimate the required actuator force of the reference aircraft, the actuation forces of the Airbus A320 high-lift system serves as a reference [16]. Hence, a single flap actuator of the Airbus A320 should be able to provide a moment of $M_{actuator,A320} = 12487 Nm$ at maximum flaps extended airspeed v_{FE}.

The actuation moment of the reference aircraft and thus the actuator force is proportional to the hinge moment caused by aerodynamic loads. For a preliminary assessment of the aerodynamic loads, the flapped wing is simplified as a kinked flat plate, and the maximum hinge moment of the flap can be calculated, see Eq. 1 [17].

$$(1) \quad M_{flap} \approx \frac{\rho_\infty}{2} \cdot v_{FE}^2 \cdot A_{flap} \cdot \bar{c}_{flap} \cdot C_{hinge,flap}$$

The hinge moment coefficient can be calculated by using Eq. 2 [17]. The parameter α represents the angle-of-attack, whereas γ defines the deflection angle of the flap.

$$(2) \quad C_{hinge,flap} = C_{hinge,\alpha} \cdot \alpha + C_{hinge,\gamma} \cdot \gamma$$

For the assumption of incompressible flow at approach speed and a wing with infinite span, the derivatives $C_{hinge,\alpha}$ and $C_{hinge,\gamma}$ can be calculated from the ratio of the mean flap-chord to the mean wing-chord [17]. The moments are calculated for each flap of the reference aircraft and the Airbus A320, see Table 5.

TABLE 5. Calculated hinge moments on the flaps.

Hinge moment	Ref. Aircraft	Airbus A320	Unit
Inboard Flap	-8156	-10883	Nm
Outboard Flap	-8784	-10767	Nm
Total	-16940	-21650	Nm

Since the moments between inboard and outboard flap differ only slightly, no further distinction is made within this study. Finally, the maximum actuator moment originally estimated is scaled using Eq. 3.

$$(3) \quad M_{actuator,REF} = M_{actuator,A320} \cdot \frac{\sum M_{flap,REF}}{\sum M_{flap,A320}}$$

In the case of linear actuators (EHA/EMA) the required maximum actuator force F and actuator power P can be calculated in general with Eqs. 4 and 5.

$$(4) \quad F_{actuator} = M_{actuator} \cdot l_{lever}$$

$$(5) \quad P_{actuator} = F_{actuator} \cdot v_{actuator}$$

The parameter l_{lever} represents the lever arm and $v_{actuator}$ the required actuation speed. However, since it is intended that the actuator should be able to hold the flap in position or actuate it in case the second actuator fails, the required actuator force should be doubled. The resulting main requirements for linear actuators are summarized in Table 6.

TABLE 6. Actuation requirements for linear actuators.

Requirement	Value	Unit	Requirement	Value	Unit
Actuator stroke	520	mm	Actuation force	60	kN
Actuation speed	17	mm/s	Actuation power	1.19	kW

At this point, only low-frequency deployment of the flaps is considered. The frequency response of the actuation system is important when high-frequency control functions are considered (e.g. gust load control). Consequently, if the multifunctional trailing-edge flaps should enable high-frequency control functions, the frequency response characteristics should be stated accordingly.

4 HIGH-LIFT SYSTEM ARCHITECTURES

In this contribution, only the trailing edge actuation system is considered. The actuation system of the leading-edge devices is very similar. Nevertheless, the potential of functional enhancement of the devices at the leading edge is more limited, compared to the trailing edge devices of the wing. Based on the outlined requirements for high-lift systems in chapter 3, two types of actuation architectures are developed for the reference aircraft. Firstly, a conventional architecture with a centrally actuated transmission shaft is modelled and serves as a reference. Secondly, three concepts of advanced system architectures with distributed electric drives are developed.

4.1 Reference System Architecture

The Reference System Architecture (RSA) represents a generic actuation system, similar to the architecture shown in the background section. The trailing edge flaps are actuated by a mechanical transmission shaft, which is actuated over a central Power Control Unit (PCU), see Figure 9. The right-hand side (not shown) will be symmetric and powered by the same drive shaft to prevent any asymmetry.

RGB	Right-angle Gearbox
DGB	Drive Gearbox
KGB	Kink Gearbox
PCU	Power Control Unit

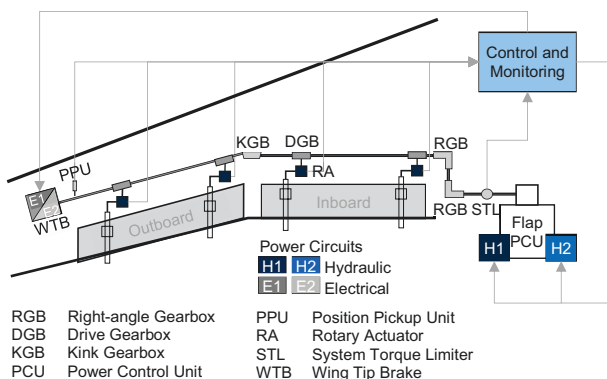|	
PPU	Position Pickup Unit
RA	Rotary Actuator
STL	System Torque Limiter
WTB	Wing Tip Brake

FIGURE 9. Schematic of the Reference System Architecture (RSA) with conventional transmission shaft system.

The inboard flap and outboard flap are each driven by two individual Rotary Actuators (RAs). The RAs are connected via a mechanical transmission shaft to the central PCU. The PCU drives the shaft over two individual hydraulic motors, which are supplied by two different hydraulic circuits (H1 and H2). The gearboxes are required for the routing of the transmission shaft around the main landing gear boxes and through the wing. A power-off Wing Tip Brake (WTB) in

each wingtip holds the drive shaft and thus the inboard and outboard flaps in position. The brake is also required in the event of a failure, e.g. a rupture of the mechanical transmission shaft, to hold position of the flaps.

The Position Pickup Units (PPUs) on the drive shaft transmit the actual position of the flap actuation system to the control and monitoring unit. Furthermore, a System Torque Limiter (STL) is integrated at the drive shaft close to the PCU. Furthermore, each RA has an integrated torque limiter (not shown). In the event of a jam or sluggishness within a RA or the drive shaft, the control and monitoring unit receives signals from the torque limiters. The control and monitoring unit is dual redundant with two lanes to control and monitor the actuation system.

4.2 Distributed System Architectures

The Distributed System Architecture (DSA) is independent from the implemented actuator types due to the power-by-wire concept. Therefore, for each DSA concept, either EMAs, EHAs or a combination of both can be chosen for actuation. The impact of the different actuator types on system safety and required redundancy levels is considered during analysis and evaluation. For all three DSA concepts, two electrical power circuits are available to supply the electrical motor and brakes. Nevertheless, the electrical motor must not necessarily be supplied by two redundant electrical power circuits, as it is shown in the schematics of the DSA concepts in Figure 10-12. Detailed analysis within the PSSA reveals, if single or dual redundant power supply is required.

Distributed System Architecture 1

The initial design of the developed Distributed System Architecture 1 (DSA1) with distributed electric drives is illustrated in Figure 10. For the DSA1, the transmission shaft system and the centrally located PCU are removed. All drive stations can be driven individually by the respective actuator (EHA or EMA). Consequently, each drive station requires a brake, position sensors and signal connections, to prevent any uncommanded motion of the inboard or outboard flaps.

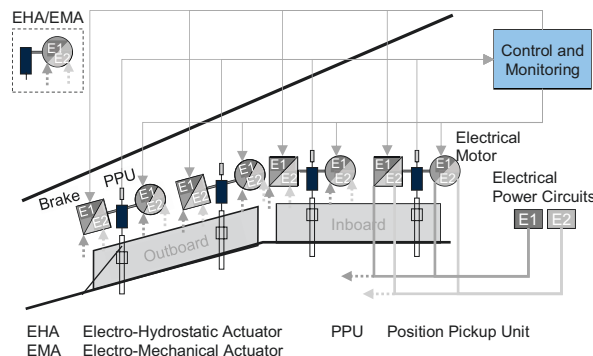|			
EHA	Electro-Hydrostatic Actuator	PPU	Position Pickup Unit
EMA	Electro-Mechanical Actuator		

FIGURE 10. Distributed System Architecture 1 (DSA1).

Two different electrical power circuits (E1 and E2) supply the electrical actuators and the brakes on each flap. The control and monitoring unit ensures a safe system operation. The main tasks are to control the distributed motors and brakes and to detect and prevent any system malfunc-

tions. For example, the position sensors can detect uncommanded asymmetry or motion of the flaps. Furthermore, the control and monitoring unit assures synchronous deployment of the actuators on each flap to prevent skewing.

Distributed System Architecture 2

The Distributed System Architecture 2 (DSA2) is an evolution of DSA1. As shown in Figure 11, the two drive stations of each inboard or outboard flap are now connected via a local drive shaft. This ensures a synchronously deployment of both actuators. For each flap, only one brake and on position sensor are required. In the case of a failure of one electric actuator, the other actuator can drive the flap in a degraded mode. In comparison to DSA1, a significant number of components and wires can be removed. Furthermore, the tasks of the control and monitoring unit are reduced.
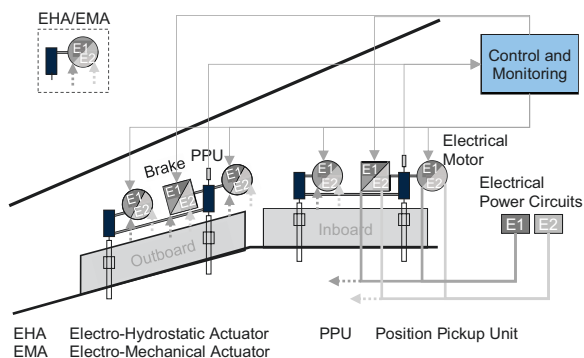

| EHA | Electro-Hydrostatic Actuator | PPU | Position Pickup Unit |
| EMA | Electro-Mechanical Actuator | | |

FIGURE 11. Distributed System Architecture 2 (DSA2).

Distributed System Architecture 3

Another evolutionary step is represented by DSA3, see Figure 12. The two actuators of each flap are powered by only one electrical motor. To provide redundancy, the motor should have multiple individual electrical power sources. The Geared Rotary Actuator (GRA) is driven via a mechanical transmission shaft by the same electrical motor.
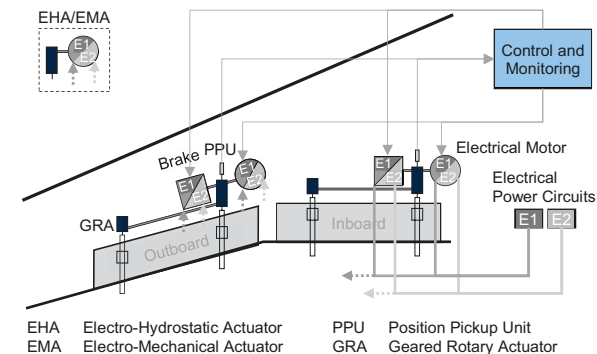

| EHA | Electro-Hydrostatic Actuator | PPU | Position Pickup Unit |
| EMA | Electro-Mechanical Actuator | GRA | Geared Rotary Actuator |

FIGURE 12. Distributed System Architecture 3 (DSA3).

5   EVALUATION AND RESULTS

The Reference System Architecture (RSA) and the three Distributed System Architecture (DSA1-3) are designed for the reference aircraft presented in section 3.1. In this chapter, the RSA and DSAs are evaluated in terms of system reliability and safety, system mass, and direct operating costs.

5.1   System Safety and Reliability Estimation

During the FHA, the aircraft level functions of the high-lift system are identified and derived failure conditions are classified.

Resulting from the functional analysis, following failure conditions are described by the same fault tree and can be summarized in five main failure condition groups:

1) Flap system runaway
   - Flap system runaway above v_{FE}
   - Flap system runaway below v_{FE}
   - Uncommanded retraction of flap system

2) Loss of operation capability of the flap system
   - Loss of extension/retraction capability

3) Failure in position indication of the flap system
   - Loss of position indication
   - Misleading position indication

4) Flap asymmetry
   - Flap asymmetry on extension/retraction
   - Excessive asymmetry during multifunctional actuation

5) Flap skew

Finally, for all system architecture concepts a total of five fault trees are constructed.

5.2   System Mass Estimation

The total system mass is estimated by accumulating the single component masses m_i multiplied by their quantities n_i plus the sum of all length-depending masses of the linkages, see equation (6). The linkages include power supplies, mechanical transmissions and signal lines. The mass is estimated over the component length l_j and a mass-factor per unit length w_j. An additional mass-fraction of 2% is considered by adding the factor f_{add}.

$$(6) \quad m_{system} = f_{add} \cdot \left(\underbrace{\sum_{i=1} m_i \cdot n_i}_{Components} + \underbrace{\sum_{j=1} l_j \cdot w_j}_{Linkages} \right)$$

System Components

The individual masses of all components of each system architecture are derived from literature review or estimated. Components that are not sized to aerodynamic loads or conditions, are assumed to be the same size and mass as the components on similar transport aircraft (A320 and B737). The mass of components that are dependent of aerodynamic loads and actuation aspects are scaled with the flap hinge moments of the estimated actuation requirements shown in Table 6.

System Linkages

In addition to the component masses, the masses of all linkages, including electric wiring, hydraulic pipes and mechanical shafts are estimated. The main data for the mass estimations are shown in the appendix.

5.3 Direct Operating Costs Estimation

Over the full life-cycle of a transport aircraft, the operating costs comprise most of the total expenses by the operator. The Direct Operating Costs (DOCs) are variable costs directly caused by operating the aircraft, which include

- Crew costs
- Depreciation for all system components
- Fuel costs, due to engine-power offtakes and system mass
- Direct Maintenance Costs (DMC) of the system
- Spare Holding Costs (SHC) to keep the system in service
- Costs due to Delays and Cancelations

The DOCs of the developed system architectures are estimated by using the DOC_{SYS}-Method of Scholz [18,19]. In this study, the DOCs are calculated per year and aircraft. Furthermore, it is assumed that the operator's fleet consists of 10 aircraft and each aircraft performs 1000 flights a year with a typical flight time of 3.6 hours. The crew costs are usually not affected by different system architectures and are assumed to remain constant for all system architectures.

5.4 Overall System Results

The overall results of the safety and reliability estimations are shown in Figure 13. It can be observed, that the safety requirements for the catastrophic failure conditions of flap runaway and flap asymmetry are fulfilled ($< 10^{-9}$). Furthermore, DSA2 and DSA3 also fulfill the safety requirements regarding flap skew ($< 10^{-5}$), due to the mechanical shaft that enables the synchronization of the two actuators on each flap. The remaining safety requirements are not fulfilled exactly. However, the failure probabilities are in the order of the safety requirements.
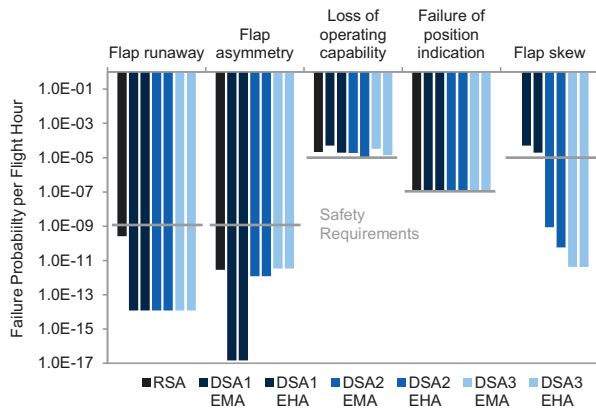

FIGURE 13. System failure probability estimation results.

The results of the system mass estimations are visualized in Figure 14. In terms of total mass, all DSA – except of DSA3 with EHAs – show a reduced mass compared to the reference architecture RSA. This is mainly due to the fact, that a lot of the heavy components of the transmission shaft system (e.g. gearboxes) are not required. The reason why DSA3 with EHAs has a significantly higher mass than all other system architectures results from the safety analysis. In this architecture, the EHAs need to be utilized in a dual redundant tandem or parallel configuration to achieve the

desired safety requirements regarding operability. However, the mass penalty for the DSA3 with EMAs due to this effect is less, since only dual redundant power drive electronics with little mass impact are required.
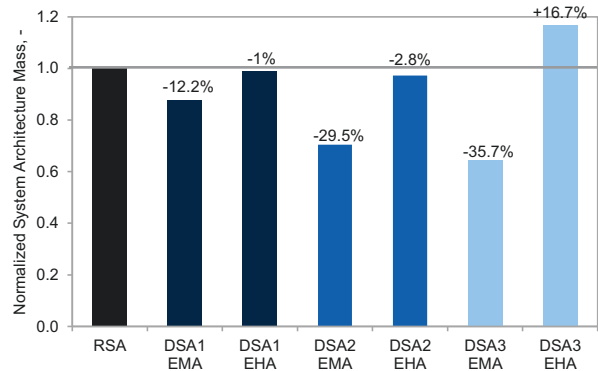

FIGURE 14. Normalized system architecture mass results.

In general, it can be observed that the architectures with EHAs have a higher overall system mass than the architectures with EMAs. This is even true for DSA1, where the EMA requires a dual redundant electrical power supply, while the EHAs are single redundant. The reason is that all EHAs need their own integrated hydraulic system with pump, fluid and reservoir.

The comparison of the overall system operating costs is visualized in Figure 15. All DSAs with distributed electric drives – with exception of DSA3 with EHAs – show lower operating costs than the reference architecture (RSA). Again, the operating costs are due to the fully dual redundant actuators, leading to high fuel costs due to the higher mass, as well as higher SHCs and DMCs compared to the other system architectures. In summary, the overall system results show an advantage of the DSA concepts with EMAs regarding lower overall system masses.
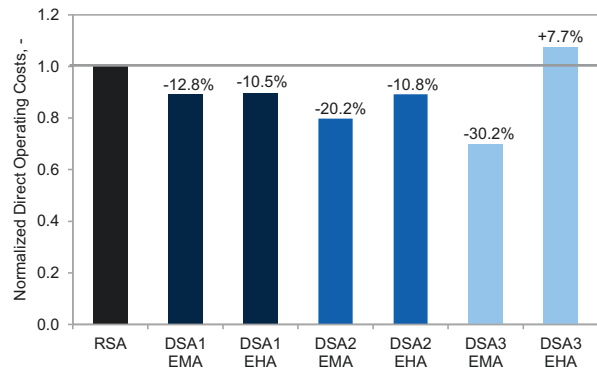

FIGURE 15. Normalized direct operating cost results.

The best overall results – regarding system safety, overall mass and operating costs – are achieved by the DSA3 with EMAs. Based on the made assumptions in this study, this architecture offers the best potential for an optimized architecture design. However, a major drawback of the EMAs is the possible jam of the mechanical actuator, and may limit the flexibility according the functional enhancement of the trailing-edge flaps. For high-lift control, such a failure mode can be accepted for the flap system as shown in the safety analysis.

Nevertheless, it should be considered, that the EHAs have better characteristics to enable high-speed actuation of the trailing-edge flaps to provide additional functions. If further advancement regarding the functional enhancement and multifunctional use of the trailing-edge flaps should be achieved, the concepts DSA1 and DSA2 with EHAs should be chosen. Both show similar results of overall system mass and direct operating costs, with slightly advantages of the DSA2 concept.

5.5 Detailed System Results

To better understand the overall system results, a detailed view and breakdown of the results of the most promising architectures – the DSA2 with EHAs and DSA3 with EMAs – are discussed and compared to the Reference System Architecture (RSA). Figure 16 shows the breakdown of the system masses (top) and the direct operating costs (DOCs) per year (bottom) of the three different architectures.

The relative mass breakdown of the RSA shows the different components and their impact on the overall system mass. The actuators, motors, brakes (49%) and the mechanical shaft system (36%) have the largest shares of the estimated total system mass of 213kg. The overall system mass breakdown of the DSA concepts are clearly different. The actuators, motors and brakes have the largest share of the overall system masses of 89% (DSA2) and 84% (DSA3) respectively. Furthermore, the relative share of the electrical wiring (3%) is considerably higher than for the RSA.

The relative breakdown of the DOCs per year of all three concepts are quite similar, regarding fuel costs, costs due to delay and cancelation and deprecation. For example, the fuel costs have shares of 40% (RSA), 36% (DSA3) and 43% (DSA2) of the overall DOCs. Major differences can be seen in the Direct Maintenance Costs (DMCs). The DMCs of the RSA have share of 17%, whereas the DSA2 and DSA3 concept show shares of 9% and 10% respectively.

6 CONCLUSION

In this study, three different high-lift system concepts with distributed electric drive architectures (DSA1-3) are developed. The distributed electrical drives will offer the capability for implementation of additional control functions for high-lift control devices. Furthermore, to meet the requirements of More-Electric Aircraft (MEA), two types of electrical actuators – the Electro-Mechanical Actuator (EMA) and the Electro-Hydrostatic Actuator (EHA) – are considered. To have a basis for the analysis and evaluation, a reference aircraft is defined, including a reference high-lift system architecture (RSA) with a conventional transmission shaft system.

The DSA1 consists of two drive stations for each inboard and outboard flap and can be driven individually by the respective actuator (EHA or EMA). For the DSA2, the two drive stations of each inboard or outboard flap are now connected via a local drive shaft to ensure a synchronously deployment of both actuators on each flap. This allows to reduce a significant number of components compared to DSA1. For the concept of DSA3, each flap is actuated by one EHA/EMA and a geared rotary actuator driven via a mechanical transmission shaft.

The system concepts are evaluated according to system reliability and safety, system mass, and direct operating costs. The best overall results are achieved by the DSA3 with EMAs. However, a major drawback of the EMAs is the possible actuator jamming and the possibly too low actuation speeds for functional enhancement of the trailing-edge devices. Consequently, for the multifunctional use of the trailing-edge flaps, concepts DSA1 and DSA2 with EHAs should be considered, which show similar results in system mass and direct operating costs.
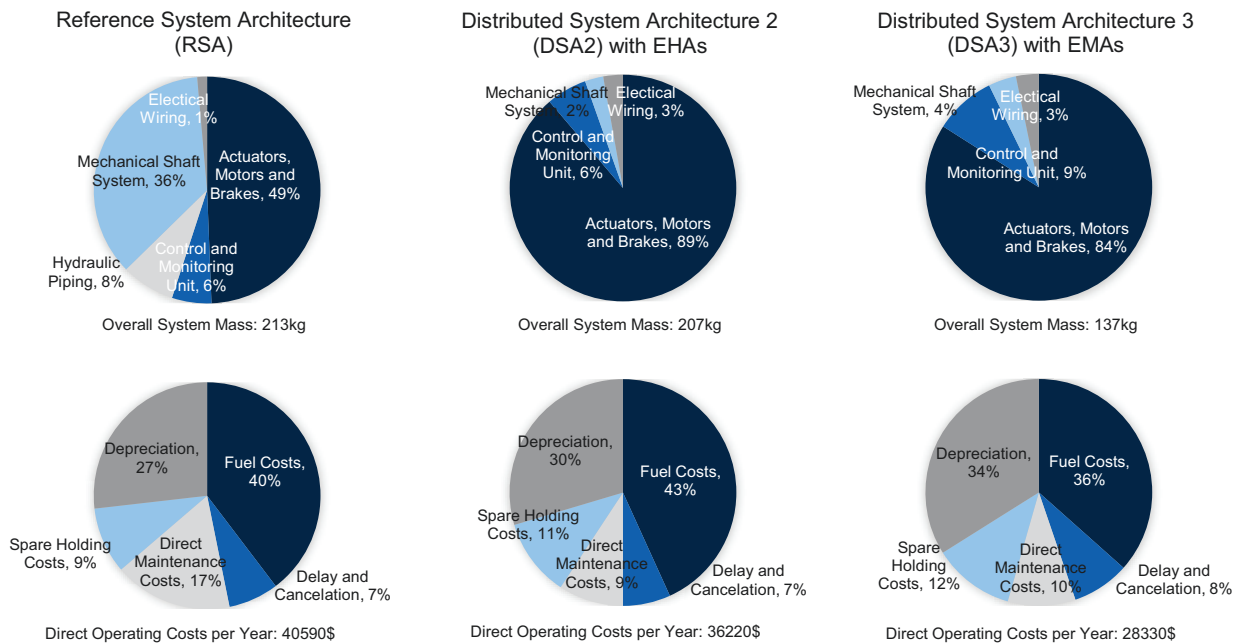

FIGURE 16. Detailed results of the system mass and cost estimation for the Reference System Architecture (left), the istribute System Architecture 2 with EHAs (middle) and the Distribute System Architecture 3 with EMAs (right).

REFERENCES

[1] M. Recksiek, "Advanced High Lift System Architecture with Distributed Electrical Flap Actuation," in *Proceedings of the 2nd International Workshop on Aircraft System Technologies*: *March 26 - 27, 2009, Hamburg, Germany,* O. von Estorff, Ed., pp. 49–60, Shaker, Aachen, 2009.

[2] T. Lampl, D. Sauterleute, and M. Hornung, "A Functional-Driven Design Approach for Advanced Flight Control Systems of Commercial Transport Aircraft," in *Proceedings of the 6th International Workshop on Aircraft System Technologies*: *February 21-22, 2017, Hamburg, Germany,* O. von Estorff and F. Thielecke, Eds., pp. 3–12, Shaker, Herzogenrath, 2017.

[3] S. L. Botten, C. R. Whitley, and A. D. King, "Flight Control Actuation Technology for Next-Generation All-Electric Aircraft," *Technology Review Journal*, pp. 55–68, 2000.

[4] I. Chakraborty, D. N. Mavris, M. Emeneth et al., "A methodology for vehicle and mission level comparison of More Electric Aircraft subsystem solutions: Application to the flight control actuation system," *Proceedings of the Institution of Mechanical Engineers, Part G: Journal of Aerospace Engineering*, vol. 229, no. 6, pp. 1088–1102, 2015.

[5] J.-C. Derrien, "Electromechanical Actuator (EMA) Advanced Technologies for Flight Controls," in *International Council of Aeronautical Sciences (ICAS) - 28th International Congress of the Aeronautical Sciences*, International Council of Aeronautical Sciences (ICAS), Brisbane, Australia, 2012.

[6] J. W. Bennett, B. C. Mecrow, A. G. Jack et al., "A Prototype Electrical Actuator for Aircraft Flaps," *IEEE Transactions on Industry Applications*, vol. 46, no. 3, pp. 915–921, 2010.

[7] M. Christmann, S. Seemann, and P. Jänker, "Innovative Approaches to Electromechanical Fligh Control Actuators and Systems," May 2010.

[8] T. W. Wild, *Transport category aircraft systems*, IAP, Inc, Casper, WY, 1990.

[9] G. Dargel, H. Hansen, J. Wild et al., "Aerodynamische Flügelauslegung mit multifunktionalen Steuerflächen," September 2002.

[10] D. Reckzeh, "Multifunctional Wing Moveables: Design of the A350XWB and the Way to Future Concepts," in *29th Congress of the International Council of the Aeronautical Sciences,* International Council of Aeronautical Sciences, Ed., St. Petersburg, Russia, 2014.

[11] I. Moir and A. G. Seabridge, *Aircraft systems*: *Mechanical, electrical, and avionics subsystems integration*, Wiley, Chichester, West Sussex, England, Hoboken, NJ, 2008.

[12] SAE ARP4754, "Guidelines for Development of Civil Aircraft and Systems," 12/21/2010.

[13] Rudolph, Peter K. C., "High-Lift Systems on Commercial Subsonic Airliners," September 1996.

[14] D. Zaccai, *Design Framework for Trailing Edge High-Lift Systems*: *A Knowledge Based Engineering Application,* Master Thesis, Delft University of Technology, August 2014.

[15] European Aviation Safety Agency (EASA), *Certification Specifications and Acceptable Means of Compliance for Large Aeroplanes CS-25*: *CS-25*, May 2017.

[16] M. Chaves-Vargas, *Aufbau einer Datenbasis zur Modellierung konventioneller Hochauftriebssysteme,* Master Thesis, RWTH Aachen, January 2010.

[17] H. Schlichting and E. A. Truckenbordt, *Aerodynamik des Flugzeuges*: *Zweiter Band: Aerodynamik des Tragflügels (Teil II), des Rumpfes, der Flügel-Rumpf-Anordnung und der Leitwerke*, Springer Berlin Heidelberg, Berlin, Heidelberg, 2001.

[18] D. Scholz, "Betriebskostenschätzung von Flugzeugsystemen als Beitrag zur Entwurfsoptimierung," in *Deutsche Gesellschaft für Luft- und Raumfahrt (DGLR) - Deutsche Luft- und Raumfahrt Kongress 1995*, S. 50-61, Deutsche Gesellschaft für Luft- und Raumfahrt (DGLR), Bonn, 1995.

[19] D. Scholz, "DOCSYS - A Method to Evaluate Aircraft Systems," in *Bewertung von Flugzeugen*: *Workshop - DGLR-Fachausschuß S2 Luftfahrtsysteme,* D. Schmitt, Ed., Garching, 1998.

[20] J. W. Bennett, *Fault Tolerant Electromechanical Actuators for Aircraft,* PhD Thesis, Newcastle University, November 2010.

[21] H. Qi, Y. Fu, X. Qi et al., "Architecture Optimization of More Electric Aircraft Actuation System," *Chinese Journal of Aeronautics*, vol. 24, no. 4, pp. 506–513, 2011.

[22] K. R. McCullough, *Design and Characterization of a Dual Electro-Hydrostatic Actuator,* Master Thesis, McMaster University, January 2011.

APPENDIX

A.1 Fault Tree Analysis

Table A.1 provides a summary of the assumed component failure rates per flight hour for high-lift system architectures.

Table A.1 Component and system failure rates [20,21].

Component/System	Failure mode	Failure rate per Flight Hour
Control and monitoring lane	No command	$3.30 \cdot 10^{-4}$
	Erroneous command	$3.30 \cdot 10^{-4}$
Position pickup unit	No signal	$2.00 \cdot 10^{-6}$
	Erroneous signal	$2.00 \cdot 10^{-6}$
Brake	No engagement	$2.80 \cdot 10^{-6}$
	No release	$2.40 \cdot 10^{-6}$
Torque limiter	No function	$2.00 \cdot 10^{-6}$
Mechanical actuator	Disconnect	$2.00 \cdot 10^{-8}$
	Jam	$1.10 \cdot 10^{-6}$
Hydraulic motor (PCU)	No drive	$1.20 \cdot 10^{-3}$
	runaway	$1.20 \cdot 10^{-3}$
Gearbox	Jam	$5.70 \cdot 10^{-7}$
Mechanical shaft	Rupture	$9.30 \cdot 10^{-7}$
Bearing	Sluggishness	$1.10 \cdot 10^{-6}$
Hydraulic power system	Loss of power	$1.00 \cdot 10^{-4}$
Electrical power system	Loss of power	$1.20 \cdot 10^{-5}$

Since no reliable data is yet provided for the failure rates of EHAs and EMAs, failure models via Fault Tree Analysis (FTA) are modeled, using basic component failure rates from the work of Bennet [20]. The results of the overall failure rates of the electrical actuator used in this study are shown in Table A.2.

Table A.2 Failure rates of the electrical actuators.

Actuator	Failure mode	Failure rate per Flight Hour
Electro-Hydrostatic Actuator (EHA) single-redundant	Loss of output	$1.96 \cdot 10^{-4}$
Electro-Hydrostatic Actuator (EHA) dual-redundant (actuator)	Loss of output	$3.94 \cdot 10^{-6}$
Electro-Mechanical Actuator (EMA) single-redundant	Loss of output	$1.07 \cdot 10^{-4}$
Electro-Mechanical Actuator (EMA) dual-redundant (electric)	Loss of output	$2.78 \cdot 10^{-6}$

A.2 Mass Estimation

Data from literature review [4,22] are used to estimate the actuator mass for Electro-Mechanical Actuators (EMAs) and Electro-Hydrostatic Actuators EHAs, see Figure A.1. On the right, the characteristics of single-redundant EMAs and the linear regression line are shown. To account for dual-redundant control electronics, the regression line is shifted upwards, considering an estimated increase of +25% in overall actuator mass. The results of the linear regression for EHAs is shown in Figure A.1 on the left. Here, literature data for single-redundant and dual-redundant (tandem actuator) could be found.

Finally, the actuator masses for the required maximum actuation force of 60kN calculated in section 3.2 can be determined from the graphs, see Table A.3.
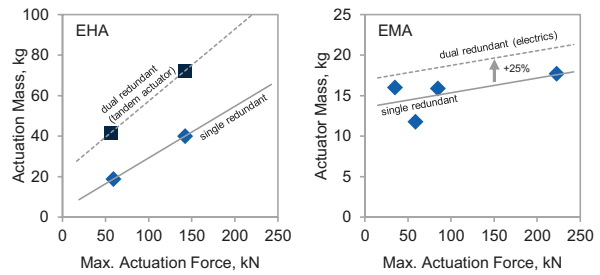

FIGURE A.1. Maximum actuation force against actuator mass of EHAs and EMAs.

Table A.3 Masses and number of installed actuators.

Actuator (max. force = 60kN)	Mass	Unit	DSA1	DSA2	DSA3
Electro-Hydrostatic Actuator (EHA) single-redundant	21.7	kg	8	8	-
Electro-Hydrostatic Actuator (EHA) dual-redundant (actuator)	45.8	kg	-	-	4
Electro-Mechanical Actuator (EMA) single-redundant	14.7	kg	-	8	-
Electro-Mechanical Actuator (EMA) dual-redundant (electric)	18.4	kg	8	-	4

Other essential component masses are given in Table A.4. The concepts with mechanical drive shafts (DSA2 and DSA3) additionally require joints and bearings, to enable wing bending and thermal extensions during flight.

Table A.4 Masses and number of installed components.

Components	Mass	Unit	DSA1	DSA2	DSA3
Brakes	1.66	kg	8	4	4
Mechanical drive shaft (inboard)	0.60	kg	-	2	2
Mechanical drive shaft (outboard)	0.49	kg	-	2	2
Joint and bearings (total)	3.16	kg	-	1	1
Geared rotary actuator	8.16	kg	-	-	4

Masses of electrical wiring are estimated over approximated lengths of the connections and the American Wire Gauge (AWG) convention. In this study, following types of wires are used for different applications, see Table A.5

Table A.5 AWG wiring used for the system architectures.

Electrical wiring	AWG	Diameter	Unit
Control wiring to - Brakes - Motors - Sensors	20	0.762	mm
Power supply to - Brakes	16	1.270	mm
Power supply to - Electric actuators	14	1.524	mm

Since most of the mass is contributed to the copper leads, the density of copper will be used and a factor of 1.2 is applied to account for insulation, tie-downs and connectors.